OPSE metrology system onboard of the PROBA3 mission of ESA

Loreggia, D., Bemporad, A., Capobianco, G., Fineschi, S., Focardi, M., et al.

D. Loreggia, A. Bemporad, G. Capobianco, S. Fineschi, M. Focardi, F. Landini, G. Massone, G. Nicolini, M. Pancrazzi, M. Romoli, I. Cernica, M. Purica, E. Budianu, C. Thizy, E. Renotte, J. S. Servaye, "OPSE metrology system onboard of the PROBA3 mission of ESA," Proc. SPIE 9604, Solar Physics and Space Weather Instrumentation VI, 96040F (7 October 2015); doi: 10.1117/12.2191591

SPIE.

Event: SPIE Optical Engineering + Applications, 2015, San Diego, California, United States

OPSE metrology system on board of the PROBA3 mission of ESA

D. Loreggia[a], A. Bemporad[a], G. Capobianco[a], S. Fineschi[a], M. Focardi[b], F. Landini[b], G. Massone[a], G. Nicolini[a], M. Pancrazzi[b], M. Romoli[c], I. Cernica[d], M. Purica[d],E. Budianu[d], C. Thizy[e], E. Renotte[e], J.S. Servaye[e].

a. INAF – Astrophysical Observatory of Turin, Via Osservatorio, 20, 10025 Pino Torinese, Torino, Italy
b. INAF – Astrophysical Observatory of Arcetri, Largo Enrico Fermi, 5, 50125 Firenze*, Italy*
c. University of Florence – Dep. of Physics and Astronomy, Largo E. Fermi, 22, 50125 Firenze, Italy
d. IMT – National Institute for Research and Development in Microtechnologies, 126A Erou Iancu Nicolae Street, 077190, Bucharest, Romania
e. CSL – Centre Spatial de Liège, Liège Science Park, 4031 Angleur (Liège), Belgium

ABSTRACT

In recent years, ESA has assessed several mission involving formation flying (FF). The great interest in this topics is mainly driven by the need for moving from ground to space the location of next generation astronomical telescopes overcoming most of the critical problems, as example the construction of huge baselines for interferometry. In this scenario, metrology systems play a critical role. PROBA3 is an ESA technology mission devoted to in-orbit demonstration of the FF technique, with two satellites, an occulter and a main satellite housing a coronagraph named ASPIICS, kept at an average inter-distance by about 144m, with micron scale accuracy. The guiding proposal is to test several metrology solution for spacecraft alignment, with the important scientific return of having observation of Corona at never reached before angular field. The Shadow Position Sensors (SPS), and the Optical Position Emitters Sensors (OPSE) are two of the systems used for FF fine tracking. The SPS are finalized to monitor the position of the two spacecraft with respect to the Sun and are discussed in dedicated papers presented in this conference. The OPSE will monitor the relative position of the two satellites and consists of 3 emitters positioned on the rear surface of the occulter, that will be observed by the coronagraph itself. By following the evolution of the emitters images at the focal plane the alignment of the two spacecrafts is retrieved via dedicated centroiding algoritm. We present an overview of the OPSE system and of the centroiding approach.

Keywords: Solar Corona, Coronagraph, Formation Flying, Optical Metrology, Space Technology, LED, Centre of Gravity, Centroid.

1. Introduction

The formation flying - F^2 - concept for the PROBA3/ASPIICS mission is described in detail in other paper of this conference [1]. Here we remind shortly some aspects to have a complete idea of the different step of the FF acquisition and of the metrology systems involved, with particular focus on the Optical Sensors Emitter System - OPSE.

The PROBA3 project focuses on the verification, test, and validation of many technological aspects that are critical to maintain the formation flying geometry of two separate and independent spacecrafts during all mission lifetime (2yrs). To this end, some metrology concepts, alignment procedures and control systems will be operate during different moments of the mission. All these metrology subsystems will work to realize the relative alignment of the two spacecrafts and the absolute alignment of the F^2 with respect to the Sun, from centimeter to micron level. In this way, it will be possible to finalize the scientific objective of the mission: to perform high spatial and temporal resolution imaging of the Solar Corona in the visible waveband from 1.08 to about $3R_{sun}$ by mean of a dilute Coronograph with the telescope housed on one

Solar Physics and Space Weather Instrumentation VI, edited by Silvano Fineschi, Judy Fennelly, Proc. of SPIE Vol. 9604, 96040F · © 2015 SPIE
CCC code: 0277-786X/15/$18 · doi: 10.1117/12.2191591

satellite (Coronagraph Spacecraft - CSC) and the external occulter on the other spacecraft (Oculter Spacecraft - OSC), at a fixed distance of 144.3m.

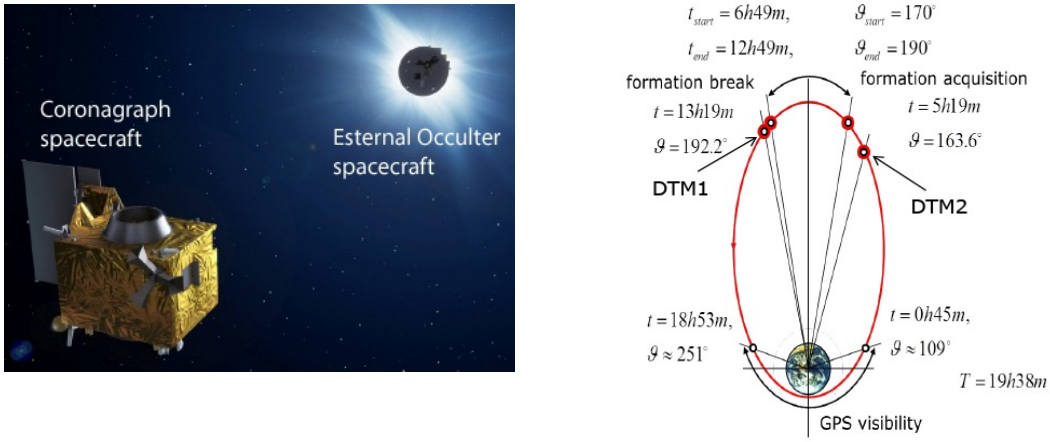

***Figure 1**: Two spacecraft picture and the orbit description*

In table 1 the F^2 orbital main parameters are reported:

Table 1: PROBA 3 orbital parameters

Parameter	Value
Perigee height	600 Km
Apogee height	60530 Km
Semi-major axis	36943 Km
Eccentricity	0.811
Orbit Inclination	59°
RAAN	84°
AoP	188°
Orbital Period	19h38m

The optimal alignment, when Coronagraph observation are done, must be maintained over 6hrs across the apogee orbital position with an error in the relative and absolute lateral positioning down to 50μm (best case realized using the SPS).

2. Metrology subsystem

Each spacecraft will board different formation flying metrology subsystems that will be tested and validated. The operation of the metrology systems is planned as an acquisition chain that starts from the more coarse alignment at cm level (GPS) up the finest one, at micron level (HAM - High Accuracy Metrology).

The relative positioning of the two spacecrafts in these phases of the operation are controlled via a radio frequency link (RFL) that will be in charge to have the relative positioning monitored quite constantly and to realize the best conditions for HAM. The RFL alignment is in loop with the maneuvers of the two spacecrafts so to correct any significant variation of the relative orbit.
Our focus is on one of the high accuracy metrology sub-system that are expected to operate at the end of the alignment chain: the Optical Positioning Sensor Emitters or OPSE.
The OPSE with the Shadow Positioning Sensors [2,3] are expected to guaranty the most accurate alignment of the External Occulter centre with the Coronagraph pupil centre, where it is positioned the Payload Reference System (OPSE) and of both the payload with respect to the Sun (SPS). This is mandatory to have the Sun perfectly obscured. The expected accuracy for the OPSE is of the order of 300μm (3σ) for lateral positioning and of 20cm for longitudinal positioning (3σ).

3. Description of OPSE system

The OPSE consists of three light emitting caps, each cap housing 4 LEDs and positioned at different distance from the centre of the OSC, within a diameter ≤ 400mm, and at different inter distance (≤ 75mm). Of the four LEDs mounted in each cap, only two are operated; the duplicity of each couple of emitter has been decided mainly for redundancy proposes. In Fig. 2, a possible representation of the OPSE positioning on the External Occulter (EO) payload is shown.

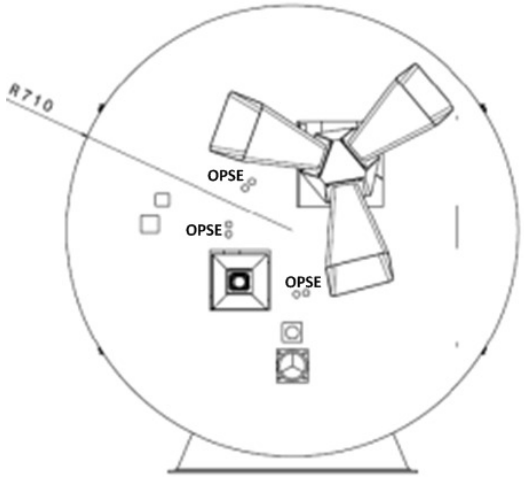

Figure 2 : *OPSE positioning on the OSC*

The LEDs will emit light within a cone angle of 6° and with a wavelength in the range [540-570]nm. The monochromatic photons will be collected by the Coronagraph telescope and imaged on the same focal plane as the scientific images over a 2048x2048 pixels CMOS sensor [4]. The design of the coronagraph is shown in Fig.3.

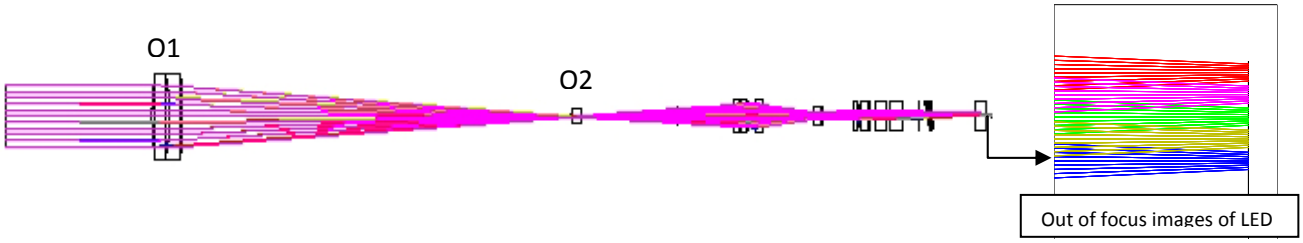

Figure 3: *Optical layout of the ASPIICS coronagraph. Detail of the out of focus image of the OPSE LED*

Because the CI is designed to image the Sun Corona at 1AU, the images of each OPSE LED (at 144.3m) will be out of focus. If we consider the test case of LED at [0, 100, 200]mm, we have the out of focus spot diagrams shown in the figure:

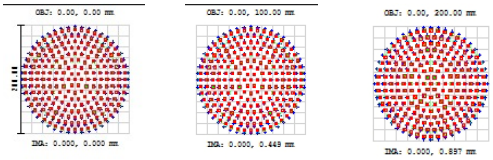

(0 ; 0)mm (0 ; 100)mm (0 ; 200)mm

RMS (GEO) Spot diagram radius(μm) over the fields and the wavelengths				
λ/Field	540 nm	555nm	570nm	590nm
[0;0]mm	69.91 (90.78)	67.79 (87.76)	66.91 (86.11)	69.58 (89.15)
[0;100]mm	69.90 (90.88)	67.79 (87.84)	66.91 (86.14)	69.58 (89.19)
[0;200]mm	69.88 (90.97)	67.78 (86.90)	66.90 (86.16)	69.58 (89.24)

Figure 4: *Spot diagrams for the considered positions*

The LEDs are assumed as point-like sources because the dimension of the emitting head is very small (~5mm) compared to the ISD (144.3m). The out of focus PSFs at the considered positions will be read with a detector area at least of 40x40 pixels (400x400μm), in order to have the full envelope well mapped for optimal centroiding.

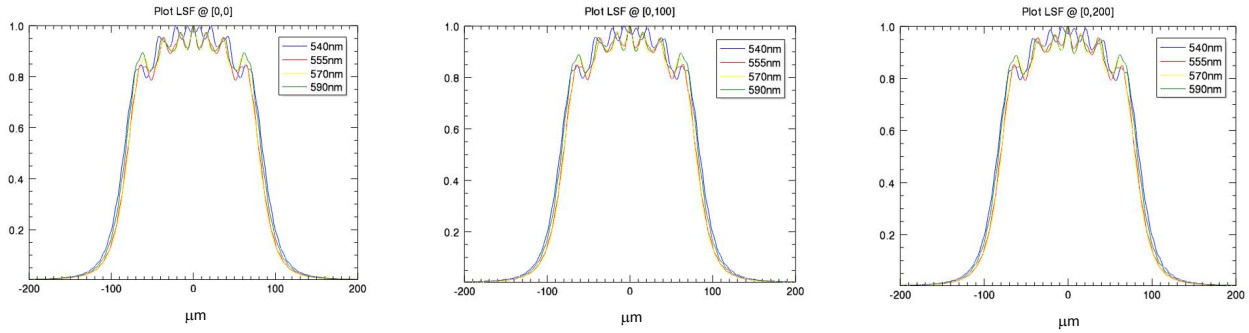

Figure 5: *LSF at the considered field height for wavelengths [540,555,570,590] nm*

The variation of the LSF over the fields and over the wavelength is very small with the assumed sampling (or larger).

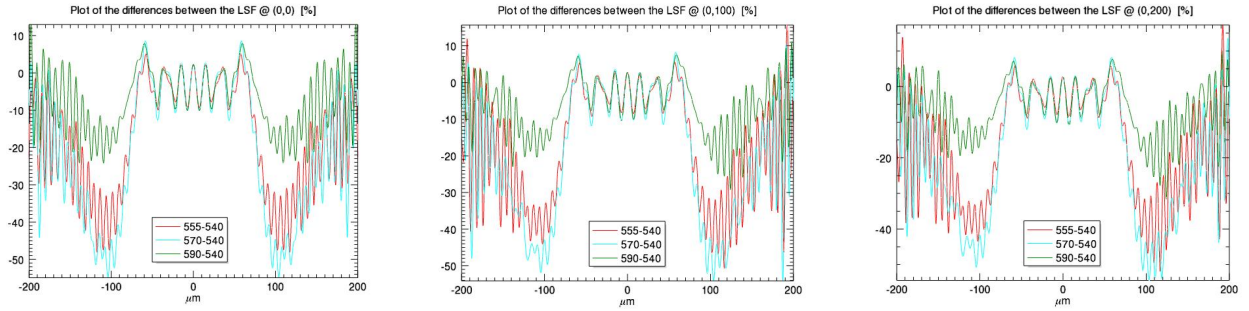

Fig. 6 *Differences between the LSF over the wavelengths and the field*

In Fig.6 it can be seen how the contribution of the field height manifests as an asymmetry of the LSF that becomes clear above 100µm. The difference tents to decrease beyond 200µm. Considering a 40x40 pixels wide window for the centroiding might by useful to care correctly of the system asymmetries contribution.

As a further test, we looked at the trend of the total flux on the OPSE PSF integrated over the considered sampling window:

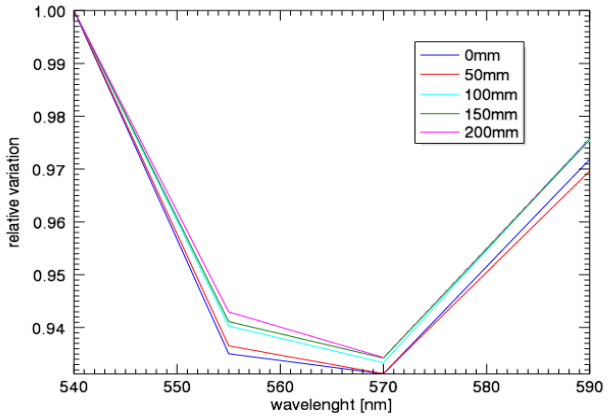

Figure 8: *Representation of the variation of the flux with λ and field height .Values are normalized to the flux @ Field =[0.0 ; 0.0]*

The maximum variation over the wavelengths is about 7%, while is quite negligible over the field.

4. Internal Occulter

As in all the coronagraph design, an Internal Occulter – IO stops the light diffracted by the EO. The IO is expected to be realized by an evaporation procedure of optically dense material on the O2 plane surface, that looking at the entrance pupil (Fig.3), with an hole in the centre to let the OSPE beams to cross (central part of the O2 surface is let transparent).

The dimension of this hole strictly depends on the scale of the O1 lens. The current design make the spot diagrams of the OPSE on the surface where the IO is expected, to spread over an area with a maximum radius of 0.3 $R_{\odot}$, in agreement with mission requirements (occultation in the range from 0.3 to 1.08 Solar radii), as reported in Table 3:

Table 3*: Dimension of the polychromatic image at IO*

Polycromatic Image of OPSE at IO			
	Max spot radius [μm]	Radial image position [mm]	Radial image position [$R_{\odot}$]
[0 ; 0]mm	1.89	[0.0 ; 0.0]	[0.0 ; 0.0]
[0 ; 100]mm	1.89	[0.0 ; -0.23]	[0.0 ; -**0.15**]
[0 ; 200]mm	1.86	[0.0 ; -0.46]	[0.0 ; -**0.30**]

Because of the tolerance due to the uncertainty requirement for the lateral movement we can set the location of the OPSE <200mm. On the counterpart, we verified that the defocusing due to the required longitudinal accuracy range (±20cm @3σ) does not affect the dimension of the spots and their position significantly.

5. System efficiency

The total optical efficiency of the system is given by the efficiency of the optical elements that compound the CI and the efficiency of the band pass filter and of the polarimetric optics. The contribution of these terms are shown in the next tables:

Table 4: *Optics efficiency*

Throughput values for the bandpass filter and the polarimetric optics	
Bandpass filter *	60 %
Quarter wave retarder	95 %
LCVR	90 %
Linear Polarizer	67 %
TOTAL	**34%**

Throughput values for the ASPIICS optics	
570 nm	83.54 %
555 nm	83.42 %
540 nm	82.73 %
TOTAL	**82.99 %**

* *Reference values for of METIS with a 580-640 nm bandpass*

The sensor will be employed for ASPIICS is the same of the EUI instrument onboard the Solar Orbiter payload [4] with a QE that is > 50% over the waveband [540-570]nm. We consider as reference a value of QE = 50% so that summarizing the contribution to the CI system due to the efficiency of the optics, the band pass filter, the polarimeter, and the detection efficiency within the reference wavelengths range, we get:

Table 6: Overall throughput values for the ASPIICS (optics + CMOS QE) [%]

λ	BP filter polar. Optics	Optics	QE	TOTAL
570 nm	34	83.54	50	**14.20**
540 nm	34	82.73	50	**14.06**

6. Radiometric budget

The typical emission power (@25°C) of the candidate LED is about 0.3mW and the emission angle is α= ±6° so that the emission solid angle is $\Omega_{LED} = 2\pi\,[1-\cos(\alpha)]$ = **0.034 str**. On the other hand, the CI pupil at the occulter subtends a solid angle:

$$\Omega_{pupil} = \frac{A_{pupil}}{D^2} = \frac{\pi \cdot (25\text{mm})^2}{(144300mm)^2} = 9.4 \cdot 10^{-8}\ \text{str} \qquad (1)$$

The effective collecting volume is obtained by dividing the pupil solid angle and the LED solid angle.

Now, the OPSE will operate at -117° and the values for the power emission refer to the emission at ambient temperature (25°C). Consider that the emitting energy of the LEDs changes with the operation temperature. Typically it increases while the temperature decreases as :

$$\text{Power}(@25°C) * [1 - (\Delta T * TC)] \quad (2)$$

where ΔT is the temperature difference and TC is the thermal coefficient that is of the order of -0.6%/°C.
This means that for the expected variation ΔT=142°C (from 25° to -117°) we will experience an increasing of the output power of about 85%.
After being collected by the CI pupil, the light from OPSE will suffer of the optics absorption and the detector QE reported in Tab. 6, that will reduce the amount of photoelectrons read by the detector to about 14% of the incoming power. So, we can retrieve the final count of photoelectrons *per* second as:

$$N\_phel = Power_{(mW)} * [Photon\_Energy(\lambda)]^{-1} * \Omega_{pupil} * 1.85 * (\Omega_{LED})^{-1} * SYS\_Eff \quad (3)$$

Sampling the OPSE PSF with a window of 40 x 40 pixels, with reference wavelengths [540; 570]nm, we get a preliminary evaluation of the power balance and a representative value of SNR:

***Table 7**: Photon Budget*

Lambda [nm]	Emission angle [°]	Power [mW]	Phel/sec	Phelt/sec/pixel	SNR
540	6	0.30	$6.0 \cdot 10^8$	374987	612
570	6	0.30	$6.3 \cdot 10^8$	395819	628

7. Accuracy requirement at focal plane

Because we need sensitivity along both the coordinate axes, as basic assumption for all the centroiding solution, we plan to consider the Line Spread Function along the two reference axes, LSF_x and LSF_y so that a PSF binning procedure both along the row and along the column, must be considered.

7.1 Lateral movements accuracy

Being EFL = 734.7mm the effective focal length of the CI (plate scale 2.81arcsec) and ISD = 144.3m, the accuracy requirement for lateral displacement measurement (3σ) of **300μm** [AD1] is conjugated at FP with a PSF shift centroiding accuracy :

$$\sigma_{Centroid} = 0.3 * EFL / ISD = \mathbf{1.5\mu m} \quad (4)$$

that corresponds to about $1/7^{th}$ of pixels (sub-pixel sensitivity).

7.2 Longitudinal movements accuracy

With the current CI design, we check that the accuracy on the focal plane for longitudinal movements of the OSC of 210mm (3σ), we have:

***Table 9**: Longitudinal sensitivity (3σ) @ plate scale 2.81 arcsec*

OPSE position range [mm]	Sensitivity to long. shift of ±210 mm [3σ]
[0 – 100]	[0.00 ; 0.73] μm
[100 - 200]	[0.73 ; 1.47] μm

In Tables 9, we see that at 3σ the sensitivity is slightly lower than 1μm when the LEDs are located at a distance from the centre of the OSC of about 100mm. We fix the centroiding requirement at FP to 1μm (≤ 3σ) i.e. 1/10th of pixels, with the proposal to test for the goal of 0.5μm (~1σ).

8. Centroiding algorithms

The requirement for accuracy of the order of 1/10th of pixel is not critical because many centroiding algorithms discussed in the literature [5,6,7] can be used to obtain such level of accuracy, with the typical flux from the OPSE LED . We plan to employ the simple *Centre of Gravity* algorithm being very reliable and efficient for direct access the PSF movements and to get backward analysis of the F^2 configuration. Beside, during the testing phases, we plan to realize a fitting procedure that will be primarily used to crosscheck the CoG performances and, by second, to get morphology evolution of the image, under *a priori* known perturbations. This will yield to build a dataset of analytical terms that will combine the PSF modification (position, width, skewness,...), with the OSC movement and the geometry of the system as a whole.

8.1 Center of Gravity

The CoG algorithm applies to each spot image I, the following function:

$$CoG = \left(\frac{\sum_i x_i I_i}{\sum_i I_i}; \frac{\sum_i y_i I_i}{\sum_i I_i} \right) \qquad \sigma^2_{CoG} = \left(\frac{\sum_i (x_i - x_{CoG})^2 \cdot I_i}{\sum_i I_i} ; \frac{\sum_i (y_i - y_{CoG})^2 \cdot I_i}{\sum_i I_i} \right) \tag{5}$$

In case of negligible noise the function CoG gives, by definition, the exact position of the spot centroid. Because of reading window dimensions, to the CoG function a weighting function W is usually applied, in order correctly account of the side pixels where low flux is present. Typically, the weighting function is the PSF profile itself (pixel sampled) that gives the distribution of the power density at pixel level.

$$\mathrm{WCoG} = \mathrm{x_{CoG}} = \frac{\sum w_i x_i f_i}{\sum w_i \cdot f_i} \tag{6}$$

A PSF shift of the order of 0.1 pixel can be easily detected and we verified that the error on this measurement is very small, of the order of 10^{-3} pixel.

8.2 Numerical simulations

We run an IDL procedure that apply the CoG in Eq.6 over the LSF obtained from the parent 2D PSF that is slightly moved of a (small) random amount around its nominal centroiding position. The PSF is assumed sampled with a 40x40 pixels array (400x400μm).

The simulation was run for a sufficient large number of PSF shift values (N=100) and the standard deviation σ_{CoG} associated to each new position (shifted PSF) was considered. The CoG error is assumed to be the squared mean value of the σ_{CoG} :

$$\sigma_{CoG}^2 = e_{CoG} = \langle \left(\sum_{i=1}^{N} \sigma_{CoG} \right)^2 \rangle \quad (7)$$

For completeness, we introduced the photon noise as an additive Poissonian term in the algorithm using as reference the flux values reported in table 7. Results are presented in Table 10.

Table 10 *Centroiding error due to algorithm + photon noise*

	540nm @ 100mm $[10^{-3}\,\mu m^2]$	*540nm @ 200mm* $[10^{-3}\,\mu m^2]$	*570nm @ 100mm* $[10^{-3}\,\mu m^2]$	*570nm @ 200mm* $[10^{-3}\,\mu m^2]$
σ_{CoG}^2 *(LSF$_y$)*	15.70	15.68	16.19	16.15
σ_{CoG}^2 *(LSF$_x$)*	15.36	15.32	15.55	15.58

The error on the centroiding procedure are of the order of nanometers.

9. Conclusions

In this paper, we present the Optical Positioning Sensors Emitters metrology system on board of the PROBA-3 ESA mission that is expected to realise the completely autonomous formation flying of two independent spacecrafts. The two satellites form a diluted coronagraph (ASPIICS) with the telescope (CI) on one spacecrafts and the external occulter (EO) on the other spacecraft.

PROBA 3 is mainly a technological mission devoted to verify and validate different metrology and control systems to get two independent spacecrafts in a formation over two years of mission. Thanks to the metrology systems, ASPIICS will observe the Solar Corona extremely close to the Solar limb with a spatial and temporal resolution never reach before. The metrology sub-systems realise the alignment of the two

satellite with different accuracies, from coarse (cm) level to fine (μm) level. Between these latter sub-system category, the OPSE is expected to reach 300μm accuracy on lateral alignment and 20cm accuracy on longitudinal alignment of the two spacecrafts. The OPSE consists of three LED cups mounted on the EO facing the telescope, each one containing 4 LEDs, 2 operated during the mission and the other 2 for redundancy. The beams emitted by the LEDs are collected by the Coronagraph telescopes, as the scientific images, and the alignment is realized monitoring the image position of the LED at the CI focal plane. In this paper, an overview of the system and of the expected radiometric balance is given. The location algorithm CoG is presented and the error budget of the controiding procedure is considered. Numerical simulation show that for the case of the OPSE, that is high SNR regime, the CoG is well suited to satisfy the accuracy requirement with a very small (15nm) residual error in the centroiding procedure.

REFERENCES

[1] E.Renotte et al., "*Design status of ASPIICS, an externally occulted coronagraph for PROBA-3"*, Proc. Of SPIE Solar Physics and Space Weather Instrumentation VI, Paper 9604-8;

[2] A. Bemporad, G.Capobianco, S.Fineschi, M.Focardi, F.Landini, D.Loreggia, G.Massone, G.Nicolini, V.Noce, M.Pancrazzi, M.Romoli, S.Buckley, K.O'Neill, "*The shadow positioning sensors (SPS) for formation flying metrology on-board the ESA-PROBA3 mission***",** Proc. of SPIE Solar Physics and Space Weather Instrumentation VI, Paper 9604-9;

[3] M.Focardi, A. Bemporad, S.Buckley, K.O'Neill, S.Fineschi, M.Pancrazzi, F.Landini, V.Noce, G. Capobianco, M.Romoli, D.Loreggia, G.Massone, G.Nicolini, C.Thizy, E.Renotte, J.S.Servaye, "*Formation flying metrology for the ESA-PROBA3 Mission: the shadow position sensors (SPS) silicon photomultipliers (SiPMs) readout electronics*", Proc. of SPIE Solar Physics and Space Weather Instrumentation VI, Paper 9604-10;

[4] J. Piqueras, K. Heerlein, S. Werner, R. Enge, U. Schuhle, J. Woch, T. De Ridder, G. Meynants, B. Wolfs, G. Lepage and W. Diels, "*CMOS sensor and camera for the PHI instrument on board Solar Orbiter: evaluation of the radiation tolerance*", Proc. of SPIE High Energy, Optical, and Infrared Detectors for Astronomy V, Vol. 8453, 845314, 2012

[5] Xin Li, Shihong Zhou, Jing Ma, Liying Tan, Tao Shen, "*Centroid measurement error of CMOS detector in presence of detector noise for inter-satellite optical communications*", Proc. of SPIE, Photoelectronic detection and Imaging, Vol. 8906, 2013;

[6] O.Lardiere, R.Conan, R.Clare, C.Bradley N.Hubin,"*Compared performance of different centroiding algorithms for hig-pass laser guide star SH wavefront sensors*", Proc of SPIE Adaptive Optics Systems II, Vol. 7736, 2010;

[7] B.M.Quine, V.Tarasyuk, H.Mebrahtu, R.Hornsey, "Determining star-image location: A new sub-pixel interpolation technique to process image centroids", Computer Physics Communications 177, 700-706, 2007.